Response of doped ^{4}He droplets

Manuel Barranco
Departament d'Estructura i Constituents de la Matèria, Facultat de Física, Universitat de Barcelona, E-08028 Barcelona, Spain

E. S. Hernández
Departamento de Física, Facultad de Ciencias Exactas y Naturales, Universidad de Buenos Aires, RA-1428 Buenos Aires, Argentina
(Received 10 January 1994)

In the framework of a finite-range density-functional theory, we compute the response of ^4He_N clusters doped with a rare-gas molecule. For this purpose, the mean field for the ^{4}He atoms, their wave functions and effective quasiparticle interaction, are self-consistently calculated for a variety of particle numbers in the cluster. The response function is then evaluated for several multipolarities in each drop and the collective states are consequently located from the peaks of the strength function. The spectra of pure droplets approach those previously extracted with a similar algorithm resorting to a zero-range density functional. The spectra of doped clusters are sensitive to the presence of the impurity and are worth a future systematic investigation.

I. INTRODUCTION

Droplets of liquid ^{4}He are unique manifestations of confinement of a quantum Bose fluid to tridimensional finite shapes. Originated in supersonic beam expansions[1] or in fragmentation of bulk ^{4}He,[2] they have attracted the attention of theorists and during the last decade, a wealth of theoretical descriptions of both ground state (g.s.) properties, energy systematics, and excitation spectrum became available in the literature. Two major viewpoints can be encountered, the one founding the description of the g.s. and energy systematics on either variational[3,4] or exact[5,6] wave functions, usually by resort to a Monte Carlo algorithm, the other relying on the adoption of a density functional[7,8] within a self-consistent frame. In spite of the large accuracy of calculations based on many-body techniques, the agreement between Monte Carlo and density-functional predictions of the g.s. for ^4He_N clusters[7] has been noticed by many authors as a major achievement of density-functional theory as applied to quantum fluids.

On the other hand, a goal currently pursued by a branch of experimental research in the field of boson clusters is to ascertain the appearance of superfluid phases in these constrained finite geometries, however yet without conclusive data concerning the droplet shape.[9,10] This search for superfluidity makes evident the necessity of attaching weakly interacting probes to the bosonic droplets,[11] whose excitation spectrum, readily attainable to measurement, could bring some insight into the fluid nature of the host cluster. Among the variety of impurities that can be captured by ^{4}He fragments during their expansion, rare gases,[12,13] alkali metals and alkaline earths,[14] and SF_6 molecules[11,15] are massive enough to support a theoretical semiclassical treatment, consisting in the addition of a helium-impurity potential to the helium-helium mean field within the density-functional approach. While the interaction potential between helium and alkali atoms presents some uncertainties[16] concerning the role of the alkali electronic density, the interaction of bosonic helium atoms with rare gases[17] as well as with SF_6 molecules[18] is rather well established. However, according to recent experiments,[11,15] doubts exist regarding the location of an SF_6 impurity into a ^4He_N drop and one cannot confidently ascertain that a central helium-impurity potential will be appropriate for the description of the doped cluster.

Since in macroscopic systems a criterium for the presence of superfluidity is the existence of a finite velocity barrier for exciting the system,[19] the spectrum of excitations of the fluid is an important input for this search. One also realizes[5,6] that on the experimental side, the spectrum is more easily amenable to measurement than the g.s. and the cluster energetics, typically through the dynamic structure function arising, for example, from electron scattering on the helium clusters.[20] A major step in applications of density-functional theory to finite quantum fluids has been achieved by Casas and Stringari,[21] who computed the density-density response of ^4He_N within the random-phase approximation (RPA) for various multipolarities and atom number N in the cluster, using a zero-range density functional.[7] The agreement between the location of the collective states in Ref. 21 and those obtained with variational and microscopic approaches[6] is noticeable; however, the density-functional results usually underestimate the energy values of the collective modes to some amount. The density-density RPA response of ^3He_N clusters has also been studied by Serra *et al.*[22] and within a fluid-dynamical approach in Ref. 23.

An alternative density functional that overcomes the most current criticism posed on zero-range density functionals,[6] namely, their inability to account for finite

scale effects such as the free surface of the liquid[24,25] and drops, as well as the hard core interaction, was introduced by Dupont-Roc *et al.*[26] It combines the simplicity of the zero-range ones with the possibility of, for example, obtaining the right value for the surface tension of the liquid without explicit inclusion of gradient terms in the energy density. This finite-range density functional (FRDF) has been employed to compute a variety of g.s. and spectral properties of liquid ^{3}He,[27,28] liquid ^{4}He,[26,29–31] ^{4}He films,[32] and ^{4}He$_N$ clusters.[8] We would like to point out in passing that in their present form these FRDF do not reproduce the two-dimensional equation of state, and consequently fail to yield growing instabilities in He films on weakly attractive substrates as those found in hypernetted-chain–Euler-Lagrange calculations.[33,34]

A description of the collective spectra of bosonic helium droplets, either bare or doped with impurities, in the frame of FRDF theory, is still missing, and this is the purpose of the present work. For this sake, we have built a modified version of the FRDF in Refs. 26–30 and have computed the density-density response of the drops in the spirit of Ref. 21. Such a modified FRDF, with the proper parametrization, was already used in Ref. 35 to calculate the zero sound spectrum of liquid ^{3}He and the structure of fermionic helium clusters, together with the energetics of triplet pairing[36] in those drops. We have here considered bosonic clusters with rare-gas impurities and more specifically, calculations have been carried for Xe atoms for which the interaction potential with the helium ones is well determined.[17] A systematics in terms of other impurities can be carried out and will be the subject of a future work.

In Sec. II of this paper, we summarize the formalism employed to compute the density-density response function of the bosonic clusters, following the lines in Refs. 21, 37. Section III is dedicated to discuss the density functional here proposed as well as the corresponding self-consistent mean field and residual particle-hole (ph) interaction. The results of our calculations for several multipolarities and helium atom number are presented and analyzed in Sec. IV, while Sec. V contains the final summary and conclusions.

II. RESPONSE FUNCTION IN THE RPA

In this section we closely follow Refs. 21 and 37. The elementary excitations of the system at zero temperature are given by the poles of the density-density Green's function,[38] which in the RPA can be found by the solution of the integral equation

$$G^{\mathrm{RPA}}(\mathbf{r}_1,\mathbf{r}_2,\omega) = G^0(\mathbf{r}_1,\mathbf{r}_2,\omega) + \int d\mathbf{r}_3\, d\mathbf{r}_4\; G^0(\mathbf{r}_1,\mathbf{r}_3,\omega)\; V^{\mathrm{ph}}(\mathbf{r}_3,\mathbf{r}_4)\; G^{\mathrm{RPA}}(\mathbf{r}_4,\mathbf{r}_2,\omega). \tag{1}$$

In this equation, $G^0(\mathbf{r}_1,\mathbf{r}_2,\omega)$ is the Hartree-Fock (HF) Green's function and V^{ph} is the residual particle-hole interaction. Denoting the single-particle (sp) energies and wave functions by e_n and ϕ_n, respectively, for a Bose system at zero temperature one has

$$G^0(\mathbf{r}_1,\mathbf{r}_2,\omega) = N\sum_n \left\{ \frac{\phi_0^*(\mathbf{r}_1)\phi_0(\mathbf{r}_2)\phi_n^*(\mathbf{r}_2)\phi_n(\mathbf{r}_1)}{\hbar\omega - E_{n0} + i\epsilon} - \frac{\phi_0^*(\mathbf{r}_2)\phi_0(\mathbf{r}_1)\phi_n^*(\mathbf{r}_1)\phi_n(\mathbf{r}_2)}{\hbar\omega + E_{n0} + i\epsilon} \right\}, \tag{2}$$

where ϵ is a small energy parameter, N represents the number of atoms in the drop, $\phi_0(\mathbf{r})$ is the sp wave function of the Bose condensate, E_{n0} is the energy difference between sp states ϕ_n and ϕ_0, and the sum runs over all the excited HF sp states.

Once G^{RPA} has been determined, the RPA-induced (transition) density $\delta\rho(\mathbf{r})$ corresponding to a one-body excitation field $V^{\mathrm{ext}}(\mathbf{r})$ is written as

$$\delta\rho(\mathbf{r},\omega) = \int d\mathbf{r}'\, G^{\mathrm{RPA}}(\mathbf{r},\mathbf{r}',\omega)\; V^{\mathrm{ext}}(\mathbf{r}') \tag{3}$$

and one can define the associated response function $\chi(\omega)$ as

$$\chi(\omega) = \int d\mathbf{r}\; \delta\rho(\mathbf{r},\omega)\; V^{\mathrm{ext}}(\mathbf{r}). \tag{4}$$

The poles of $\chi(\omega)$ yield the elementary excitations of the system acted upon by V^{ext}, and the imaginary part of $\chi(\omega)$ is the strength function $S(\hbar\omega)$ corresponding to V^{ext}:

$$\begin{aligned} S(\hbar\omega) &= \sum_m |\,\langle m \mid V^{\mathrm{ext}} \mid 0\rangle\,|^2\, \delta(\hbar\omega - E_{m0}) \\ &= -\frac{1}{\pi}\mathrm{Im}\chi(\omega)\ , \end{aligned} \tag{5}$$

where $\mid 0\rangle$ is the RPA g.s., and $\mid m\rangle$, E_{m0} are RPA excited states and energies, respectively.

The strength function presents sharp peaks at the energies of the excitations caused by the field V^{ext}, and usually more than one resonant state appears in $S(E)$. Thus a criterium is needed to ascertain which are the most collective states, a quite useful one being provided by the energy-weighted m_1 sum rule (EWSR) defined as

$$\begin{aligned} m_1 &= \sum_m E_{m0}\,|\,\langle m \mid V^{\mathrm{ext}} \mid 0\rangle\,|^2 \\ &= \int_0^\infty E\,S(E)\,dE\ , \end{aligned} \tag{6}$$

since in general, the more collective the state is, the larger the contribution of its neighborhood to the EWSR.

For $\mathbf{r}$-dependent external fields, a closed RPA expres-

sion can be worked out:[39]

$$m_1 = \frac{\hbar^2}{2m} \int d\mathbf{r}\, \rho(\mathbf{r})\, (\nabla V^{\text{ext}})^2 \ , \tag{7}$$

where $\rho(\mathbf{r})$ is the HF g.s. The comparison of the results obtained from Eqs. (6) and (7) constitutes a very stringent test on the accuracy of the numerical procedure used to calculate $\chi(\omega)$, some details of which are presented in Appendix B.

III. ^{4}He DENSITY FUNCTIONAL AND THE PARTICLE-HOLE INTERACTION

We have seen in the preceding section that the basic ingredients of the Green's function method for describing the elementary excitations in ^{4}He clusters within the RPA are the sp wave functions and energies, as well as a particle-hole interaction coming from the same He-He effective potential. This self-consistency requirement is essential for the application of the theory.[39]

Collective excitations of ^{4}He drops have been obtained within the RPA (Ref. 21) using a *local*, zero-range ^{4}He density functional whose results for g.s. properties of liquid drops compare well with other ones from microscopic methods. Finite-range and nonlocal effects are expected not to change appreciably these results[21] due to the long-wavelength character ($q \sim 0$) of the multipolar excitations there studied, which correspond to external fields of the kind $V^{\text{ext}} \sim r^l Y_{l0}(\hat{\mathbf{r}})$. Differences are expected to appear for external probes involving finite momentum transfer, such as $\exp(i\mathbf{q}\cdot\mathbf{r})$ or $j_l(qr)Y_{l0}(\hat{\mathbf{r}})$, or in the case of doped drops, due to the shell structure formed around the impurity,[8,40] which would not be predicted by a zero-range density functional.

For the present study, we have built a new FRDF largely inspired in Ref. 26 but with a hard core similar to that of Pines' polarization potentials[41] (see also Ref. 35). Accordingly, the density functional is written as

$$E[\rho] = \int d\mathbf{r}\, \mathcal{E}(\rho)$$

$$= \int d\mathbf{r} \left\{ \frac{\hbar^2}{2m} \sum_i |\, \nabla\phi_i(\mathbf{r})\, |^2 + \frac{c}{2}\rho(\mathbf{r})[\tilde{\rho}(\mathbf{r})]^{\gamma+1} \right.$$

$$\left. + \frac{1}{2}\rho(\mathbf{r}) \int d\mathbf{r}\,'\rho(\mathbf{r}\,')V(|\, \mathbf{r}-\mathbf{r}\,'\,|) \right\}. \tag{8}$$

In this equation, $\tilde{\rho}(\mathbf{r})$ is the coarse-grained density introduced in Ref. 26:

$$\tilde{\rho}(\mathbf{r}) = \int d\mathbf{r}\,'\,\rho(\mathbf{r}\,')\mathcal{W}(|\, \mathbf{r}-\mathbf{r}\,'\,|) \ . \tag{9}$$

The weighting function $\mathcal{W}(|\, \mathbf{r}\,|)$ reads

$$\mathcal{W}(|\, \mathbf{r}\,|) = \begin{cases} \frac{3}{4\pi h^3} & \text{if } |\, \mathbf{r}\,| < h, \\ 0 & \text{otherwise} \ . \end{cases} \tag{10}$$

The finite-range interaction consists of a screened Lennard-Jones (LJ) potential:

$$V(r) = \begin{cases} 4\epsilon_{\text{LJ}} \left[\left(\frac{\sigma}{r}\right)^{12} - \left(\frac{\sigma}{r}\right)^{6} \right] & r \geq \sigma, \\ b_{\text{LJ}} \left[1 - \left(\frac{r}{\sigma}\right)^{8} \right] & r \leq \sigma. \end{cases} \tag{11}$$

The height b_{LJ} of the core is fixed so that the bulk properties of the finite-range functional be the same than those of the zero-range functional out of which it is derived. It yields[35]

$$b_{\text{LJ}} = \frac{33}{8} \left[\frac{8}{9}\epsilon_{\text{LJ}} + \frac{b}{4\pi\sigma^3} \right]. \tag{12}$$

We shall take the parameter values[26]

$$\epsilon_{LJ} = 10.22 \text{ K},$$
$$\sigma = 2.556 \text{ Å},$$
$$h = 2.377 \text{ Å},$$
$$b = -888.81 \text{ K Å}^3,$$
$$c = 1.04554 \times 10^7 \text{ K Å}^{3(\gamma+1)},$$
$$\gamma = 2.8.$$

At zero temperature, all particles belong to the Bose condensate and we have

$$\rho(\mathbf{r}) = \sum_i |\, \phi_i(\mathbf{r})\, |^2 = N \,|\, \phi_0(\mathbf{r})\, |^2 \ . \tag{13}$$

The kinetic energy density can thus be written as

$$\tau(\mathbf{r}) = \sum_i |\, \nabla\phi_i(\mathbf{r})\, |^2 = N \,|\, \nabla\phi_0\, |^2 = \frac{1}{4}\frac{(\nabla\rho)^2}{\rho}. \tag{14}$$

Varying $E[\rho] - \sum_i e_i \,|\, \phi_i\, |^2$ with respect to ϕ_i^* yields the sp wave functions and energies:

$$-\frac{\hbar^2}{2m}\Delta\phi_i + \frac{\delta U}{\delta\rho}\phi_i = e_i\phi_i \ , \tag{15}$$

where $U[\rho]$ is the potential part of Eq. (8). It is worth noting that the sp energy corresponding to the Bose condensate ϕ_0 is the chemical potential of the drop.

We collect in Table I the results obtained solving Eq.

TABLE I. Ground-state results for several $^4\text{He}_N$ drops obtained solving Eq. (15). The values corresponding to the homogeneous liquid are also given.

N	E/N (K)	μ (K)	r_0 (Å)	ρ_0 (10^{-2} Å^{-3})
8	-0.47	-1.26	3.71	1.09
20	-1.40	-2.62	2.87	1.82
40	-2.27	-3.54	2.60	2.09
70	-2.97	-4.16	2.48	2.19
112	-3.51	-4.40	2.41	2.23
168	-3.94	-4.74	2.36	2.26
240	-4.28	-5.00	2.33	2.27
330	-4.56	-5.20	2.31	2.27
728	-5.16	-5.61	2.27	2.27
∞	-7.15	-7.15	2.22	2.19

(15) for several ^{4}He clusters. In this table, ρ_0 is the central density of the drop, μ the chemical potential, and E/N the energy per atom. As in Refs. 4, 7, the unit radius r_0 is defined as

$$r_0 = \sqrt{\frac{5}{3}\langle r^2\rangle}\ N^{-1/3}\ , \tag{16}$$

where $\langle r^2\rangle$ is the mean square radius of an N-atom drop.

Table I allows a sensible comparison with the results obtained from the zero-range functional.[7] The results are quite similar for large clusters, whereas for small clusters, the FRDF yields more compact and bound drops, thus improving the agreement between density functional[7] and variational Monte Carlo[4] methods. The diffusion Monte Carlo calculations of Ref. 6 for $N = 40$, 70, and 112 give stronger binding but similar $r_0(N)$.

The energies of the calculated clusters have been adjusted to a mass formula

$$E = a_v N + a_s N^{2/3} + (a_c - \tfrac{2}{9}a_s^2\mathcal{K}\rho_0)N^{1/3} + a_0\ , \tag{17}$$

where a_v is the energy per atom and $(\mathcal{K}\rho_0)$ the compressibility of the liquid at saturation density ρ_0.[7] It gives $a_s = 17.77$ K, $a_c = 7.25$ K, $a_0 = -28.0$ K, and a surface tension of 0.287 K Å^{-2}, to be compared with the experimental value 0.274 K Å^{-2}.[42] The latter one coincides by construction with the theoretical value of Ref. 7, and with that obtained in Ref. 26. At present, the commonly accepted experimental value is 0.256 K Å^{-2}.[43] The small disagreement between theory and experiment could be fixed readjusting the parameters ϵ_{LJ} and σ in Eq. (11). As we have indicated in Ref. 35, insofar as one is interested in extracting droplet properties, there is no fundamental reason for keeping the free-atom values in the liquid regime.

Following Ref. 8, the impurity has been treated as a classical object; i.e., we have added to $\mathcal{E}$ in Eq. (8) the term

$$V_I(\mathbf{r})\rho(\mathbf{r})\ , \tag{18}$$

where $V_I(\mathbf{r})$ is the helium-impurity potential, so that the effect of the term Eq. (18), is simply to add $V_I(\mathbf{r})$ as an external field in Eq. (15). Furthermore, we consider the impurity to lie at the center of the drop.

Figure 1 shows the g.s. density of pure ^{4}He$_{40}$ and ^{4}He$_{728}$ drops (solid lines), both with and without a Xe impurity at the center (dashed lines). The structure and binding energy systematics of doped ^{4}He have been throughly discussed by Dalfovo[8] using the density functional of Ref. 26. The results here obtained for these quantities using the present FRDF follow the same systematics, although our functional yields weaker binding. For example, we find that the chemical potential of Xe

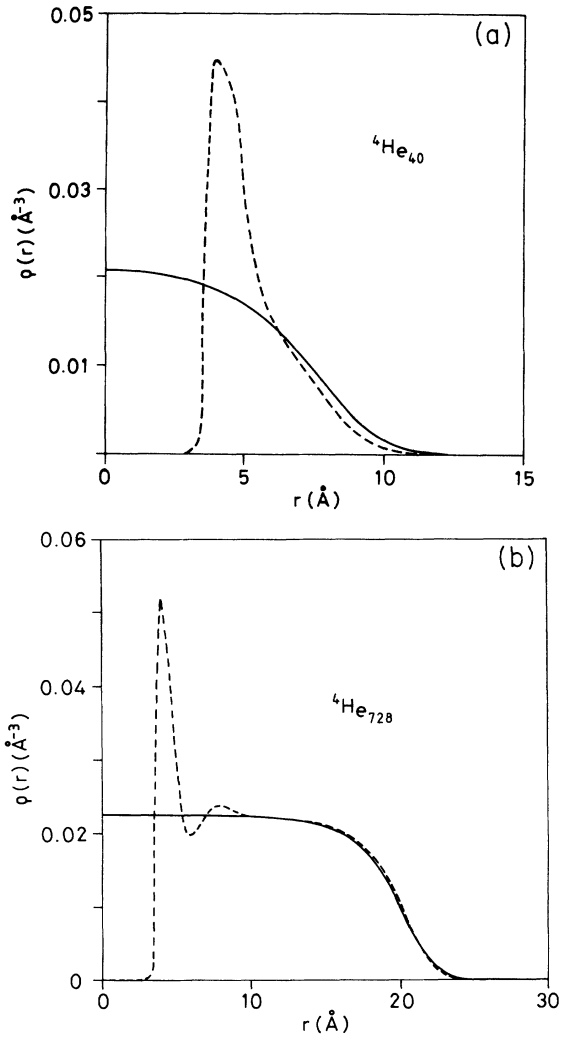

FIG. 1. Density profiles of pure ^{4}He$_{40}$ (a) and ^{4}He$_{728}$ (b) drops (solid lines), and of the same drops with a Xe atom at the center (dashed lines).

$$\mu_{Xe} = E(^4\mathrm{He}_N + \mathrm{Xe}) - E(^4\mathrm{He}_N) \tag{19}$$

approaches a value of ~ -250 K when N increases, whereas Dalfovo has found ~ -300 K for this quantity.

Within the theory of quantum liquids, the particle-hole interaction V^{ph} is given by the second functional derivative of the total energy with respect to densities taken at the HF solution:

$$V^{ph}(\mathbf{r},\mathbf{r}') = \frac{\delta^2 E[\rho]}{\delta\rho(\mathbf{r})\delta\rho(\mathbf{r}')}\ . \tag{20}$$

A straightforward calculation gives

$$V^{ph}(\mathbf{r},\mathbf{r}') = V(|\,\mathbf{r}-\mathbf{r}'\,|) + \frac{c}{2}(\gamma+1)\mathcal{W}(|\,\mathbf{r}-\mathbf{r}'\,|)\,[\tilde\rho^{\gamma}(\mathbf{r}) + \tilde\rho^{\gamma}(\mathbf{r}')]$$
$$+\frac{c}{2}\gamma(\gamma+1)\int d\mathbf{r}''\,\rho(\mathbf{r}'')\tilde\rho^{\gamma-1}(\mathbf{r}'')\,\mathcal{W}(|\,\mathbf{r}-\mathbf{r}''\,|)\,\mathcal{W}(|\,\mathbf{r}''-\mathbf{r}'\,|). \tag{21}$$

It is interesting to notice that the impurity does not explicitly contribute to $V^{\rm ph}$, since Eq. (18) is linear in $\rho(\mathbf{r})$. However, it does affect $V^{\rm ph}$ throughout the changes that it introduces in the density.

IV. RESULTS

We have checked that the functional (8) reproduces the static response of homogeneous liquid ^{4}He to acceptable accuracy. This is shown in Fig. 2, where we have plotted the response $\chi^{-1}(q,\omega=0)$ for the present FRDF (solid line), as well as the results of Ref. 26 (dashed line) and the experimental points (dots) of Ref. 44.

To obtain the response to external perturbations of multipole type $V_l^{\rm ext}(\mathbf{r}) = r^l Y_{l0}(\hat{\mathbf{r}})$, one carries out an angular momentum decomposition of the functions appearing in the definition of the response function. Let us define the multipolar ph interaction $V_l^{\rm ph}(r_1,r_2)$ and response $G_l^{\rm RPA}(r_1,r_2,\omega)$ as

$$V^{\rm ph}(\mathbf{r}_1,\mathbf{r}_2) = \sum_{l,m} V_l^{\rm ph}(r_1,r_2) Y_{lm}^*(\hat{\mathbf{r}}_1) Y_{lm}(\hat{\mathbf{r}}_2), \tag{22}$$

$$G^{\rm RPA}(\mathbf{r}_1,\mathbf{r}_2,\omega) = \sum_{l,m} G_l^{\rm RPA}(r_1,r_2,\omega) Y_{lm}^*(\hat{\mathbf{r}}_1) Y_{lm}(\hat{\mathbf{r}}_2) \ . \tag{23}$$

A similar definition holds for $G_l^0(r_1,r_2,\omega)$, which can be shown to be

$$G_l^0(r_1,r_2,\omega) = \frac{N}{4\pi}\sum_n \mathcal{R}_{00}(r_1)\mathcal{R}_{00}(r_2)\cdot\left\{\frac{1}{\hbar\omega-(e_{nl}-e_0)+i\epsilon}-\frac{1}{\hbar\omega+(e_{nl}-e_0)+i\epsilon}\right\}\mathcal{R}_{nl}(r_1)\mathcal{R}_{nl}(r_2) \ , \tag{24}$$

where the radial wave function $\mathcal{R}_{nl}(r)$ is defined from $\phi_{nl}(\mathbf{r}) = \mathcal{R}_{nl}(r)Y_{nl}(\hat{\mathbf{r}})$, e_{nl} is the corresponding sp energy, and the sum runs over all the excited HF states of multipolarity l. The transition density is then naturally decomposed into multipoles $\delta\rho_l(r,\omega)Y_{l0}(\hat{\mathbf{r}})$ [see Eq. (3)], and for each of them there is an associated response function $\chi_l(\omega)$. Thus, for each multipole l the problem reduces to solving the integral Eq. (1) to obtain the corresponding $G_l^{\rm RPA}$. We give in Appendixes A and B some technical details concerning the computation of $V_l^{\rm ph}$ and $G_l^{\rm RPA}$.

Specific calculations have been carried out for the external fields $V_0^{\rm ext} = r^2 Y_{00}$ (l=0) and $V_l^{\rm ext}(\mathbf{r}) = r^l Y_{l0}(\hat{\mathbf{r}})$ with l=2 and 3. The associated m_1 sum rules are

$$m_1(l=0) = 2\frac{\hbar^2}{m}\int_0^\infty r^4\rho(r)dr, \tag{25}$$

$$m_1(l\neq 0) = \frac{\hbar^2}{2m}l(2l+1)\int_0^\infty r^4\rho(r)dr \ . \tag{26}$$

For l=1, the latter equation reduces to

$$m_1(l=1) = \frac{\hbar^2}{2m}\frac{3}{4\pi}N \ . \tag{27}$$

The l=1 mode corresponds to a translation of the drop as a whole and should lie at zero excitation energy. We have verified that this energy is always very small, in the range of 0.05–0.1 K, and that the m_1 sum rule is fulfilled in all cases to within a 5% or better.

We collect in Table II our results for the l=0, 2, and 3 multipoles corresponding to pure ^{4}He$_N$ drops with N = 40, 70, 112, 240, and 728. For l=0, the strength is shared by two states, one in the discrete ($\hbar\omega <\mid \mu_N \mid$) and another in the continuum part of the spectrum. Most of the EWSR, actually, around 75% and even more, is concentrated in the first state. When the size of the drop increases, the tendency of the l=0 strength is to concentrate in a single peak that almost exhausts the EWSR. For l=2 and 3, the strength is concentrated in a single state lying in the discrete region. The resonant states are very narrow, even those lying in the continuum region.

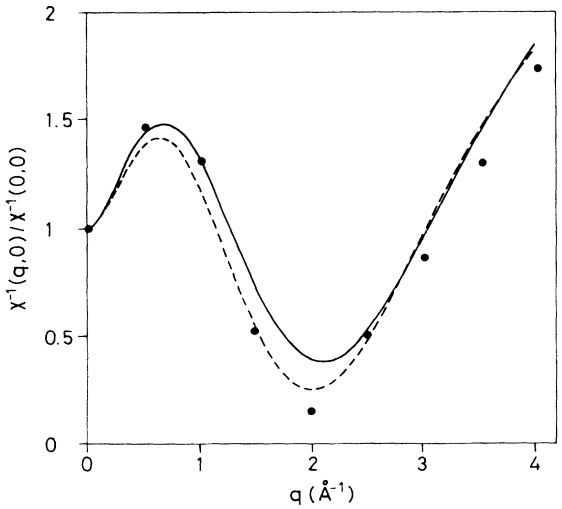

FIG. 2. Static polarizability of liquid ^{4}He. The experimental points (dots) are from Ref. 44. The solid line corresponds to the present calculation, and the dashed line to that in Ref. 26.

TABLE II. Collective energies (K) of selected ^{4}He$_N$ drops.

N	$l=0$				$l=2$	$l=3$
	$\hbar\omega_1$	% EWSR	$\hbar\omega_2$	% EWSR		
40	3.04	73	5.32	25	1.35	2.19
70	3.22	73	5.35	23	1.11	1.96
112	3.27	73	5.37	24	0.89	1.62
240	3.16	82	4.77	16	0.62	1.19
728	2.69	95	4.33	3	0.35	0.71

TABLE III. Chemical potential μ and collective energies (K) of selected ^4He_N+Xe drops.

N	μ	$l=0$						$l=2$	$l=3$
		$\hbar\omega_1$	% EWSR	$\hbar\omega_2$	% EWSR	$\hbar\omega_3$	% EWSR		
40	-3.14	3.12	20	7.34	42	11.04	36	1.89	2.58
70	-3.35	3.23	59	5.52	27	9.57	13	1.27	2.03
112	-3.65	2.92	48	4.28	20	6.61	30	0.91	1.62
240	-4.16	2.66	52	4.19	36	5.91	7	0.38	0.98
728	-4.69	2.26	63	3.24	28	4.15	7		0.32

The results of Table II are in good agreement with those of Ref. 21, thus confirming that the range of the effective interaction affects these modes only very slightly. We obtain excitation energies systematically smaller than those in Ref. 21, but rarely differing by more than 10%. In Ref. 6, the l=0 and 2 collective states of ^4He_N with N = 20, 40, 70, and 112 have been obtained using a Feynman ansatz and the diffusion Monte Carlo g.s. wave function. The collective energies are higher than the present ones, especially for the l=2 modes.

At this point, we would like to draw the attention on the different behavior of both helium isotopes regarding the position of the collective peaks in the spectrum of a drop. The monopole strength of ^3He_N lies in the continuum region, and so does the strength of quadrupole modes for small drops. This is due to the low absolute value of the chemical potential of the liquid, which is even smaller for drops due to the positive surface contributions, and to the repulsive character of the residual ph interaction. Above $N \sim 100$, the situation is reversed[22] and the quadrupole mode lies in the discrete region. Higher l modes are very fragmented and in the continuum.[45] Opposite to these facts, *all* calculations of ^4He_N spectrum so far reported yield modes that basically lie in the discrete region, even if the residual ph interaction is repulsive, the reason being the rather large value of the ^{4}He chemical potential.

We show in Fig. 1 how the presence of a Xe impurity changes the density profile. It strongly influences the spectrum of the drops, as one can see comparing the results collected in Tables II and III. The monopole mode of doped clusters is more fragmented, and for small drops, its strength lies in the continuum region (compare $|\mu|$ and $\hbar\omega_1$ in Table III). The surface $l \neq 0$ strength is still concentrated in a single mode in the discrete part that practically exhausts the EWSR, although a second l=2 and l=3 mode carrying very little strength appears for N = 40 in the continuum part of the spectrum with $\hbar\omega$ =3.5 K and 5.4 K, respectively.

The N systematics of the low surface l modes is sizably affected by the presence of the Xe atom. For small

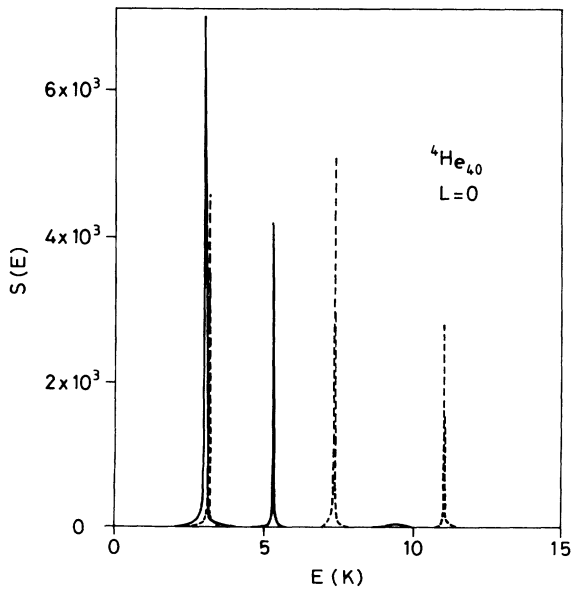

FIG. 3. Monopole strength in K^{-1}Å^4 of ^{4}He$_{40}$ (solid line) and of ^{4}He$_{40}$+Xe (dashed line).

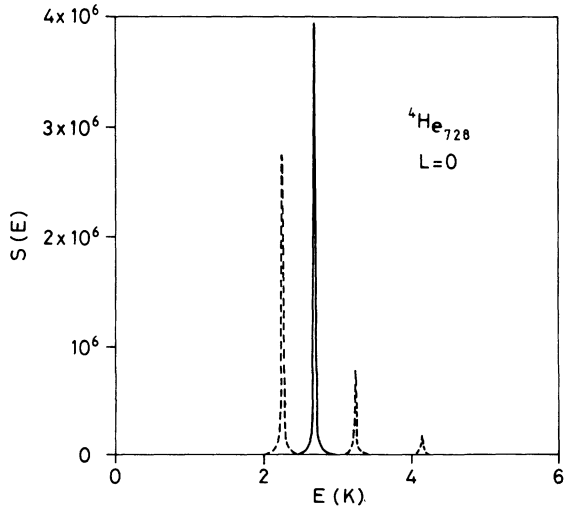

FIG. 4. Monopole strength in K^{-1}Å^4 of ^{4}He$_{728}$ (solid line) and of ^{4}He$_{728}$+Xe (dashed line).

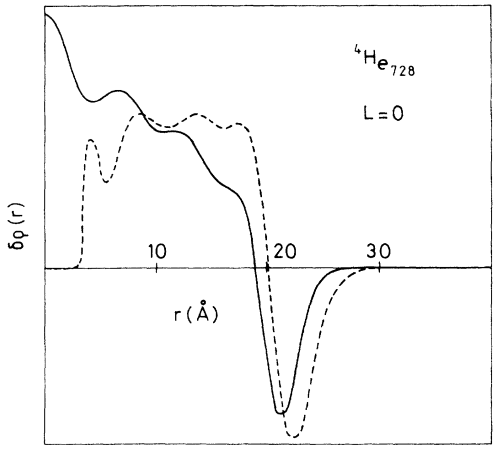

FIG. 5. Transition density $\delta\rho_0(r)$ in arbitrary scale of the first monopole collective state of $^4He_{728}$ (solid line) and of $^4He_{728}$+Xe (dashed line).

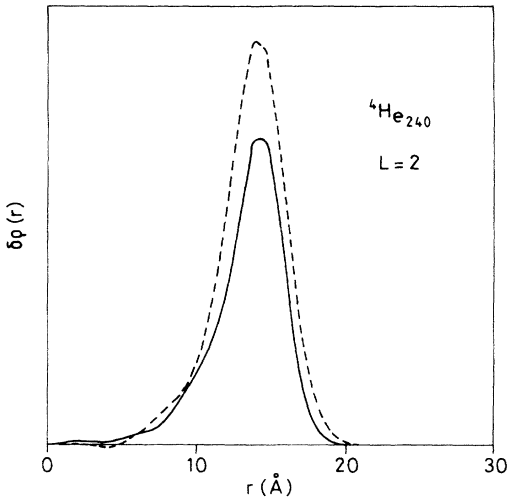

FIG. 6. Transition density $\delta\rho_2(r)$ in arbitrary scale of the first quadrupole collective state of $^4He_{240}$ (solid line) and of $^4He_{240}$+Xe (dashed line).

clusters, the peak is pushed upwards in energy, but for large clusters the energy decreases, collapsing to zero for the quadrupole mode of the $N = 728$ drop.

Figures 3 and 4 show the monopole strength corresponding to $N = 40$ and 728, respectively. The solid-line peaks are the collective states of pure drops, and the dashed-line peaks, those of the doped clusters. The volume character of monopole states is apparent from the transition density. As an example, we show in Fig. 5 the transition density $\delta\rho_0$ associated with the first l=0 state of the $N = 728$ drop (solid line) and of the $^4He_{728}$+Xe drop (dashed line). Interestingly, the monopole transition densities display persistent oscillations of the kind found in Ref. 6, which are missing in the total density.

The $l \neq 0$ transition densities are peaked at the surface, thus conferring a definite surface character to these modes, and possess almost no structure. As an example, we show in Fig. 6 the $\delta\rho_2$ transition density corresponding to the first quadrupole state of the $^4He_{240}$ and $^4He_{240}$+Xe drops.

V. SUMMARY AND OUTLOOK

In this work we have investigated the density-density response of doped ^{4}He droplets in the RPA frame. To this end, we have constructed a He-He finite range effective interaction that reproduces with reasonable accuracy the properties of the homogeneous liquid that are relevant for the problem here proposed. Single-particle wave functions and energies have been evaluated solving a mean field equation and the effective quasiparticle interaction has been extracted performing a twofold functional differentiation of the total energy.

As an example, detailed results have been obtained for the case of a Xe impurity placed at the center of the drop. We have shown that the properties of the spectrum are largely affected by the presence of the impurity, which pushes the monopole strength upwards and the low-lying surface modes downwards in energy. As a by-product, we have verified that the spectra of pure droplets exhibit strong differences with respect to those of the ^3He_N clusters,[22] concerning the energy location of the low multipolarity modes.

Both the experimental and the theoretical knowledge of these doped clusters is currently rather scarce. From the theoretical point of view, the most systematic studies have been carried out for ^4He_N drops within the density functional method.[8,46] Variational Monte Carlo calculations of ^4He_N+H_2 (Ref. 47) and path integral Monte Carlo calculations of $^3He_N^+$+Li (Ref. 48) for small N are also available, as well as variational and diffusion Monte Carlo calculations of $^4He_4$+SF_6,[49] however only concerning the properties of the g.s.

The feasibility of the density-functional method makes it possible to investigate the effect of different impurities on the energy spectrum of doped ^{3}He and ^{4}He clusters of any size. Different noble gases interact with the helium atoms with the same functional form of the potential in Eq. (18),[17] however with slightly modified scales; thus no substantial variations are to be expected with respect to the results here presented. Alkali atoms located in the center of the cluster seem to push the helium density outwards to a large extent,[8] allowing one to expect sizable effects in the collective spectra; unfortunately, the interaction field is not sufficiently well established and very qualitative features could be examined at most. Molecules of SF_6 may perhaps offer a rich perspective in view of their possibility of being captured in the surface, rather than in the center, of the cluster.[11,15] A strict treatment of these impurities would then require an anisotropic HF calculation in order to produce the major ingredients for the computation of the RPA response. A systematic study of these effects is now in progress and will be presented in a forthcoming article.

ACKNOWLEDGMENTS

We would like to thank Montserrat Casas and Franco Dalfovo for useful correspondence. This work has been partially supported by the Consejo Nacional de Inves-

tigaciones Científicas y Técnicas, Argentina (Grant No. PID 1993), and DGICYT, Spain (Grant No. PB92-0761). E.S.H. would like to thank the DGICYT, Spain, for financial support during her sabbatical stay in Barcelona.

APPENDIX A: MULTIPOLAR DECOMPOSITION OF THE PARTICLE-HOLE INTERACTION

In this appendix we sketch how to decompose the weighting function $\mathcal{W}(|\mathbf{r}-\mathbf{r}'|)$ and finite-range potential $V(|\mathbf{r}-\mathbf{r}'|)$ into multipoles.

Introducing the step function Θ, one can write

$$\mathcal{W}(|\mathbf{r}-\mathbf{r}'|) = \frac{3}{4\pi h^3}\Theta(|\mathbf{r}-\mathbf{r}'|), \tag{A1}$$

and the problem reduces to obtaining $\Theta_l(r,r')$ from

$$\Theta_l(r,r') = \frac{2l+1}{2}\int_{-1}^{+1} dx\,\Theta(h-\sqrt{r^2+r'^2-2rr'x}\,) \times P_l(x)\ , \tag{A2}$$

where $x = \hat{\mathbf{r}}\cdot\hat{\mathbf{r}}'$ and P_l is a Legendre polynomial. One can distinguish three regions.

(1) If $h < |r-r'|$, then

$$\Theta_l(r,r') = 0\ . \tag{A3}$$

(2) If $|r-r'| \le h \le r+r'$, then

$$\Theta_l(r,r') = \frac{2l+1}{2}\int_{(r^2+r'^2-h^2)/2rr'}^{+1} dx P_l(x)\ . \tag{A4}$$

(3) If $r+r' < h$, then

$$\Theta_l(r,r') = \frac{2l+1}{2}\int_{-1}^{+1} dx P_l(x) = \delta_{l,0}\ . \tag{A5}$$

To work out similar expressions for the finite-range potential $V(|\mathbf{r}-\mathbf{r}'|)$, let us call $V_{\rm LJ}(|\mathbf{r}-\mathbf{r}'|)$ its Lennard-Jones part, and $V_c(|\mathbf{r}-\mathbf{r}'|)$ its core part. Defining $u = r^2+r'^2-2rr'x$, we distinguish again three regions:

(1) If $\sigma < |r-r'|$, then

$$V_l(r,r') = \frac{2l+1}{2}\int_{-1}^{+1} dx V_{\rm LJ}(x)P_l(x) = \frac{2l+1}{4rr'}\int_{(r-r')^2}^{(r+r')^2} du V_{\rm LJ}(u)P_l[x(u)]\ . \tag{A6}$$

(2) If $|r-r'| \le \sigma \le r+r'$, then

$$V_l(r,r') = \frac{2l+1}{4rr'}\left[\int_{(r-r')^2}^{\sigma^2} du V_c(u)P_l(u) + \int_{\sigma^2}^{(r+r')^2} du V_{\rm LJ}(u)P_l(u)\right]\ . \tag{A7}$$

(3) If $r+r' < \sigma$, then

$$V_l(r,r') = \frac{2l+1}{4rr'}\int_{(r-r')^2}^{(r+r')^2} du V_c(u)P_l(u). \tag{A8}$$

All these integrals are analytical and yield $\mathcal{W}_l(r,r')$ and $V_l(r,r')$. Since, for example,

$$V(|\mathbf{r}-\mathbf{r}'|) = \sum_l V_l(r,r')P_l(\hat{\mathbf{r}}\cdot\hat{\mathbf{r}}') = \sum_{l,m}\frac{4\pi}{2l+1}V_l(r,r')Y^*_{lm}(\hat{\mathbf{r}})Y_{lm}(\hat{\mathbf{r}}')\ , \tag{A9}$$

using the preceding expressions it is straightforward to obtain $V_l^{\rm ph}$ in Eq. (22), from Eq. (21).

APPENDIX B: SOLUTION OF THE RPA INTEGRAL EQUATION

We have solved the HF equation (15) with a spatial step $\Delta r = 0.5$ Å, the same used to solve Eq. (1). For positive energy sp states, we have employed the standard trick of enclosing the droplet in a sphere of large radius R_0,[21] and have required the sp wave functions to vanish at R_0. We have taken $R_0 = 30$ Å, except for the largest cluster here studied, $N = 728$, for which we chose $R_0 = 35$ Å. We have checked that the final results are not appreciably affected by changes in Δr and R_0.

The small energy parameter ϵ in Eq. (2) was fixed to 0.01 K, and the response was obtained in energy steps of 0.01 K from zero to 10 K. Due to its special characteristics, the monopole strength of ^{4}He$_{728}$+Xe was calculated using a step of 0.02 K up to an energy of 20 K. The width at half height of the resonant states is a few times ϵ, and the number of sp states considered in the evaluation of G_l^0 was 10, which roughly corresponds to a maximum energy difference E_{n0} between 15 and 35 K depending on the size of the droplet and the angular momentum l.

For a given multipolarity, Eq. (1) has been written as

$$\int dr_4 r_4^2\left[\frac{\delta(r_1-r_4)}{r_1 r_4} - \int dr_3 r_3^2\, G_l^0(r_1,r_3,\omega)\, V_l^{\rm ph}(r_3,r_4)\right] G_l^{\rm RPA}(r_4,r_2,\omega) = G_l^0(r_1,r_2,\omega)\ . \tag{B1}$$

The integrals have been discretized using a simple rectangular integration rule, and the one-dimensional Dirac's function represented as

$$\delta(r_i-r_j) = \frac{\delta_{i,j}}{\Delta r}\ . \tag{B2}$$

Thus, (B1) becomes the following matrix equation:

$$\sum_k \mathcal{M}_{ik}\, G_l^{\rm RPA}(r_k,r_j,\omega) = G_l^0(r_i,r_j,\omega)\ , \tag{B3}$$

where

$$\mathcal{M}_{ik} = \delta_{i,k} - (\Delta r)^2 r_k^2 \sum_m r_m^2 G_l^0(r_i,r_m,\omega)V_l^{\rm ph}(r_m,r_k)\ . \tag{B4}$$

The matrix $G_l^{\rm RPA}(r_i,r_j,\omega)$ is obtained from the matrix product

$$G_l^{\rm RPA}(r_i,r_j,\omega) = \sum_k (\mathcal{M}^{-1})_{ik}\, G_l^0(r_k,r_j,\omega)\ . \tag{B5}$$

[1]H. Buchenau, E. L. Knuth, J. Northby, J. P. Toennies, and C. Winkler, J. Chem. Phys. **92**, 6875 (1990).
[2]T. Jiang and J. A. Northby, Phys. Rev. Lett. **68**, 2620 (1992).
[3]V. R. Pandharipande, J. G. Zabolitsky, S. C. Pieper, R. B. Wiringa, and U. Helmbrecht, Phys. Rev. Lett. **50**, 1676 (1983).
[4]V. R. Pandharipande, S. C. Pieper, and R. B. Wiringa, Phys. Rev. B **34**, 4571 (1986).
[5]S. A. Chin and E. Krotschek, Phys. Rev. Lett. **65**, 2658 (1990).
[6]S. A. Chin and E. Krotschek, Phys. Rev. B **45**, 852 (1992).
[7]S. Stringari and J. Treiner, J. Chem. Phys. **87**, 5021 (1987).
[8]F. Dalfovo, Z. Phys. D **29**, 61 (1994).
[9]E. G. Syskakis, F. Pobell, and H. Ullmaier, Phys. Rev. Lett. **55**, 2964 (1985).
[10]D. Eichenauer, A. Scheidemann, and J. P. Toennies, Z. Phys. D **8**, 295 (1988).
[11]S. Goyal, D. L. Schutt, and G. Scoles, J. Phys. Chem. **97**, 2236 (1993).
[12]A. Scheidemann, B. Schilling, J. P. Toennies, and J. A. Northby, Physica B **165**, 135 (1990).
[13]A. Scheidemann, J. P. Toennies, and J. A. Northby, Phys. Rev. Lett. **64**, 1899 (1990).
[14]H. Bauer, M. Beau, B. Friedl, C. Marchand, and K. Miltner, Phys. Lett. A **146**, 134 (1990).
[15]S. Goyal, D. L. Schutt, and G. Scoles, Phys. Rev. Lett. **69**, 933 (1992).
[16]S. H. Patil, J. Chem. Phys. **94**, 8089 (1991).
[17]K. T. Tang and J. P. Toennies, Z. Phys. D **1**, 91 (1986).
[18]R. T. Pack, E. Pieper, G. A. Pfeffer, and J. P. Toennies, J. Chem. Phys. **80**, 4940 (1984).
[19]M. V. Rama Krishna and K. B. Whaley, Phys. Rev. Lett. **64**, 1126 (1990).
[20]H. Buchenau, J. P. Toennies, and J. A. Northby, J. Chem. Phys. **95**, 8134 (1991).
[21]M. Casas and S. Stringari, J. Low Temp. Phys. **79**, 135 (1990).
[22]Ll. Serra, J. Navarro, M. Barranco, and Nguyen Van Giai, Phys. Rev. Lett. **67**, 2311 (1991).
[23]S. Weisgerber and P. G. Reinhard, Ann. Phys. (Leipzig) **2**, 666 (1993).
[24]D. V. Osborne, J. Phys. Condensed Matter **1**, 289 (1989).
[25]L. B. Lurio, T. A. Rabedeau, P. S. Pershan, I. F. Silvera, M. Deutsch, S. D. Kosowsky, and B. M. Ocko, Phys. Rev. B **48**, 9644 (1993).
[26]J. Dupont-Roc, M. Himbert, N. Pavloff, and J. Treiner, J. Low Temp. Phys. **81**, 31 (1990).
[27]C. García-Recio, J. Navarro, N. van Giai, and L. L. Salcedo, Ann. Phys. (N.Y.) **214**, 293 (1992).
[28]E. S. Hernández, M. Barranco, and A. Polls, Phys. Lett. A **171**, 119 (1992).
[29]E. Cheng, M. W. Cole, W. F. Saam, and J. Treiner, Phys. Rev. Lett. **67**, 1007 (1991).
[30]F. Dalfovo, J. Dupont-Roc, N. Pavloff, S. Stringari, and J. Treiner, Europhys. Lett. **16**, 205 (1991).
[31]F. Dalfovo, Phys. Rev. B **46**, 5482 (1992).
[32]E. Cheng, M. W. Cole, J. Dupont-Roc, W. F. Saam, and J. Treiner, Rev. Mod. Phys. **65**, 557 (1993).
[33]B. E. Clements, J. L. Epstein, E. Krotscheck, and M. Saarela, Phys. Rev. B **48**, 7450 (1993).
[34]B. E. Clements, H. Forbert, E. Krotscheck, and M. Saarela (unpublished).
[35]M. Barranco, D. M. Jezek, E. S. Hernández, J. Navarro, and Ll. Serra, Z. Phys. D **28**, 257 (1993).
[36]E. S. Hernández and M. Barranco, Phys. Rev. B **48**, 365 (1993).
[37]G. F. Bertsch and S. F. Tsai, Phys. Rep. C **18**, 126 (1975).
[38]A. L. Fetter and J. D. Walecka, *Quantum Theory of Many-Particle Systems* (McGraw-Hill, New York, 1971).
[39]P. Ring and P. Schuck, *The Nuclear Many-Body Problem* (Springer-Verlag, Berlin, 1980).
[40]N. Pavloff, Ph.D. thesis, University of Orsay, 1990.
[41]D. Pines, Can. J. Phys. **65**, 1357 (1987).
[42]D. O. Edwards and W. F. Saam, *Progress in Low Temperature Physics* (North-Holland, New York, 1978), Vol. VIII A, Chap. 4.
[43]M. Iino, M. Suzuki, and A. J. Ikushima, J. Low Temp. Phys. **61**, 155 (1985).
[44]R. Cowley and A. D. B. Woods, Can. J. Phys. **49**, 177 (1971).
[45]J. Navarro, Ll. Serra, M. Barranco, and Nguyen Van Giai, in *Clustering Phenomena in Atoms and Nuclei*, edited by M. Brenner, T. Lönnroth, and F. B. Malik (Springer-Verlag, Berlin, 1992), p. 83.
[46]F. Dalfovo, Z. Phys. D **14**, 263 (1989).
[47]R. N. Barnett and K. B. Whaley, J. Chem. Phys. **96**, 2953 (1992).
[48]P. Borrmann and E. R. Hilf, Z. Phys. D **26**, 5350 (1993).
[49]R. N. Barnett and K. B. Whaley, J. Chem. Phys. **99**, 9730 (1993).